Mining, Metallurgy & Exploration
https://doi.org/10.1007/s42461-024-00985-5

Maximizing the Processing of Polymetallic Concentrates via Actinide Separation and Rare Earth Retrieval

Ahmed A. Eliwa[1] · Amal E. Mubark[1] · Ebrahim A. Gawad[1] · Ahmed H. Orabi[1] · Mona M. Fawzy[1]

Received: 1 January 2024 / Accepted: 21 April 2024

Abstract
During the last decades, the growing demand for rare earth elements (REEs) has led to numerous recent studies to recover these elements from various bearing ores and wastes. Therefore, the recovery of REEs from Ras Baroud polymetallic concentrate has been investigated in the current study. Physical beneficiation for the Ras Baroud pegmatite sample was carried out, yielding a concentrate for euxenite (Y), fergusonite (Y), xenotime (Y), monazite (Ce), allanite, thorite, uranothorite, and Hf-zircon, which resulted in raising the concentrations of rare earth elements, Th, Zr, U, and Ti in the sample. Fusion digestion processes with sodium hydroxide were studied using the Conceived Predictive Diagonal (CPD) technique. The three experimental digestion groups proved the dissolution of 99.9, 95.6, 99.9, 52.5, and 0.47% for REEs, Th, U, Ti, and Zr, respectively, under fusion conditions of 723 K, 120 min, 1/1.5 ore/alkali ratio, and − 100-µm particle sizes. Fusion kinetics, isotherms, and thermodynamics were investigated using several suggested models, namely, pseudo reversible first order, uptake general model, and shrinking core model which matched well with the experimental digestion results. Selective recovery of actinide content from REE content of the digested concentrate chloride solutions was accomplished using solvent extraction with di-2-ethyl hexyl phosphoric acid. About 99.9, 99.9, and 4.2% extraction efficiencies for Th, U, and REEs were performed, respectively, using 0.3 mol/L solvent concentration in kerosene as a diluent, 1/2 organic to aqueous ratio, an aqueous pH of 0.2, and 15-min contact time. Thorium and uranium ions were stripped with sulfuric acid solution 2.5 mol/L with 94 and 98% stripping efficiency, respectively. A highly purified REE precipitate was obtained from the raffinate solutions. Zircon mineralization tailings were obtained as a by-product through the alkaline digestion process.

Keywords Physical beneficiation · Rare earths · Alkaline fusion · Modeling · Solvent extraction

1 Introduction

Many studies worldwide have revealed the presence of granite-pegmatite-hosted rare-metal mineralizations, including Nb–Ta-REE mineralization as well as Zr-Hf and U-Th mineralization [1–6]. Nb–Ta-REE mineralization has been recorded in the pegmatite bodies of Gabal Ras Baroud granite as well as in the granite itself and the surrounding stream sediments [7–11].

Ras Baroud area is considered one of the most promising areas due to the presence of several strategic and economic rare-metal and REE-bearing minerals, is located in the Central Eastern Desert of Egypt, with an area of about 106 km^2, extending along Qena-Safaga road between latitudes 26°43′21″ and 26°48′50″ N and longitudes 33°32′50″ and 33°40′08″ E. The exposed granitoid in the area under investigation is classified into two dissimilar rock units, namely, the older granitoid and the younger granites. Ras Baroud pegmatites are hosted by both older and younger granitoid, but they are often concentrated at the contact between the younger and older granites [11]. Previous beneficiation studies were performed on the rare-metal bearing minerals through gravitational concentration followed by a combination of magnetic and electrostatic separation. Froth flotation can also be used as a later or supplemental stage to achieve a cleaner product [12–17].

Great efforts have been conducted to recover rare earth elements from uranium and thorium radioactive contents from various ores. The hydrometallurgical recovery processes of the chosen elements are carried out using different techniques, with either an acidic dissolution or an alkaline

✉ Amal E. Mubark
amal_mubark2014@yahoo.com

[1] Production Sector, Nuclear Materials Authority, El Maadi, P.O. Box 530, Cairo, Egypt

Published online: 04 May 2024

dissolution. This depends on the ore nature, the element type, and the mineral type. Fusion digestion techniques for REEs and actinides as refractory minerals have been investigated successfully using alkali hydroxides. Alkali hydroxide fluxes proved effective in the digestion process of the desirable elements presented in several ores [18–21].

Using a very small number of experiments, the inventive technique "Conceived Predictive Diagonal" (CPD) was utilized in the analysis of the experimental results; this methodology resulted in workable and accurate consequences. In contrast to other methods such as the Design of Experiment (DOE) and Taguchi techniques, the CPD technique does not depend on the matrix diagonally dominant techniques or the eigenvalue principle. This technique depended on studying the parameters in a binary manner or by studying two factors simultaneously [22, 23]. By applying the CPD technique, the binary groups of experiments covered the task range skillfully, the response homogeneity was achieved, and all the alkaline digestion process factors were fully represented. The time of the digestion study was saved by employing a few steps, and the other points would not be performed. Using skills in matrices, nonlinear regression modeling, and MATLAB, the kinetics-thermodynamics relation for the alkaline digestion processes for the studied mineralization was investigated [24].

Several methods have been studied to separate rare earth elements from the content of radioactive actinides, which are usually associated together as monazite, euxenite, etc., or found together in separate minerals [25]. Separation of U and Th from REEs by precipitation was one of the most applicable separation methods; direct precipitation of U and Th using precipitating agents was widely investigated, such as sodium hydroxide, lime, hydrogen peroxide, and magnesium oxide [26–29]. Solvent extraction (SX) was the other most applicable method in the actinide separation from REEs. Acidic organophosphorus extractants, neutral organophosphorus extractants, amide extractants, amine extractants, and carboxylic acid extractants were the famous solvent extractants utilized in the differentiation between radioactive actinides and REEs [30–36]. Adsorption trials of REEs, Th, or U separately were also studied using inorganic adsorbents, organic adsorbents, and biosorbents [37–39].

The main goals of this paper were summarized in studying the optimal physical upgrading processes to attain a concentrate of high REEs, Th, U, Ti, and Zr contents. Secondly, the fusion digestion of the polymetallic concentrate using sodium hydroxide as a fluxing agent was investigated using the CPD technique. The alkaline fusion was oriented in the selective dissolution processes for the REEs, Th, and U contents leaving the Ti and Zr mineralization as a by-product for further treatment later. The optimal fluxing temperature was defined as the point at which desirable element content was selectively recovered with minimum Zr and Ti dissolution. MATLAB mathematical analyses were performed to define the activation energy, kinetics, and thermodynamics of the alkaline digestion process. Thirdly, the removal of actinides Th, and U from the REE content was studied using the solvent extraction technique with di-2-ethyl hexyl phosphoric acid in kerosene as a diluent. The solvent extraction of Th and U with D2EHPA from chloride solutions was controlled to produce raffinate solutions containing the highest REE content and without the actinides. In addition, studying the scalability of the process and environmental impact has been taken into account. Finally, the production of high-purity sediments from REEs oxide was accomplished, which achieved the main aim of this study.

2 Experimental

2.1 Materials, Reagents, and Instrumentations

Ras Baroud polymetallic concentrate resulting from physical beneficiation was used as the starting material for this study. The concentrate was analyzed mineralogically and chemically to determine its desirable elements contents (REEs, Th, U, Ti, and Zr). All chemicals and reagents were used as received without further purification. Double-distilled water (DDW) was used in all experiments in this study. The pHs of the chloride solutions were adopted using HAANA pH meter and adjusted with the concentrated HCl and NaOH solution (50%). The SEM–EDX analysis for Ras Baroud polymetallic concentrate and the outcome products was performed using scanning electron micrograph model JEOL-JSM-5600LV.

Total rare earths were instrumentally analyzed with Arsenazo III indicator at 650 nm using a single beam UV-spectrophotometer model SP-8001, Metretech Inc. Thorium was determined spectrophotometrically with Thoron indicator at 655 nm. Uranium concentration was also determined spectrophotometrically using Arsenazo III at 654 nm. On the other hand, titanium and zirconium concentrations were measured spectrophotometrically using tiron and xylenol orange at 430 and 535 nm, respectively [40].

2.2 Physical Beneficiation Stage

Physical beneficiation of the Ras Baroud pegmatite sample was carried out using a low-intensity magnetic separator (for magnetite separation), a high-intensity magnetic separator (for separating paramagnetic minerals), and a Wilfley shaking table (for rejection of associated gangue silicate minerals). After the polymetallic concentrate was obtained, a complete characterization was performed using SEM–EDX analysis to determine the mineral contents.

2.3 Fluxing Digestion Stage

A series of alkaline digestion experiments were performed on the mineral concentrate using sodium hydroxide as a fluxing agent. The polymetallic concentrate was quartered and grounded to the proper grain size before mixing with the sodium hydroxide flux in a platinum crucible and subjected to variable conditions. To treat professional data with fewer numbers of experiments with fewer numbers of experiments, a Conceived Predictive Diagonal (CPD) technique is suggested for this target. By applying the CPD technique, three groups of experiments were carried out using the binary factor study method. Fusion temperature and fusion time, ore particle size and solid-to-alkali (*S*/*A*) ratio, and fusion temperature and solid-to-alkali ratio (three binary groups) were performed under fixed conditions as presented in Table 1. Six experiments were performed in each group, which means eighteen digestion experiments with sodium hydroxide under variable and fixed conditions. In the digestion experiments, changing two variables together was carried out while maintaining the other variables at fixed values for a given set of measurements.

After each experiment, the retained crucible was allowed to cool to ambient temperature and then underwent acid dissolution using a diluted HCl solution (1/1) under 353 K, solid/acid ratio 1/10, and stirring for 30 min. The chloride slurry was filtered, washed, diluted with DDW to the flask mark, and analyzed to identify its constituents. The dissolution efficiencies for REEs, Th, U, Ti, and Zr were determined from Eq. 1:

$$\text{Dissolution efficiency } (\%) = \left(\frac{M_L}{M_o}\right) \times 100 \quad (1)$$

where M_L and M_o were REEs, Th, U, Ti, or Zr leached concentrations (mg/L) and their original concentrations in the solid (mg/g).

2.4 Dissolution Parameter Stage

The optimal digestion conditions were applied on a definite weight of the Ras Baroud polymetallic concentrate. The fused cake was washed several times with hot water to remove all undesirable gangues, namely, the dissolved phosphates, silicates, and excess sodium hydroxide. To optimize the dissolution of the studied metals, the washed cake was dried at 110 for 6 h, and then it was subjected to a series of dissolution experiments using different acids. About 1.0 g of the dried fused cake fractions was mixed with acidic portions of hydrochloric, sulfuric, nitric, and citric acids, each separately. The dissolution processes were performed using an acid concentration of 2 mol/L, solid to the acidic solution of 1/10, dissolution temperature of 253 K, and stirring for 60 min. After each experiment, the slurry was filtered, washed with DDW until it reached a definite volume, and analyzed to identify its constituents, and the dissolution efficiencies of the studied elements were calculated using Eq. 1.

2.5 Solvent Extraction Stage

A chloride feed solution was prepared using optimal fusion digestion and dissolution parameters as follows: 10 g of − 100 µm from the mineral concentrate was fused with 15 g sodium hydroxide in a platinum crucible under 723 K fusion temperature and 120 min fusion time. The fused cake was washed several times with hot water. The washed-wetted cake was spontaneously attacked with a 2 mol/L HCl with a *S*/*A* ratio of 1/10 and stirred for 60 min at a 353 K stirring temperature. The filtrated and washed solutions were adjusted with DDW until they reached 1 L. This chloride feed solution was considered the aqueous phase in the further solvent extraction processes.

The D2EHPA dissolved in kerosene was utilized as an organic phase in the subsequent lab extraction experiments. Several parameters which control the separation of actinides from REEs of the chloride feed solutions were studied. D2EHPA concentration, feed solution pH,

Table 1 Studied fusion experiments

	Group 1		**Group 2**		**Group 3**	
Exp No	Temp., K	Time, min	Ore size, µm	Ore/alkali ratio, w/w	Temp., K	Ore/alkali ratio, w/w
1	473	45	150	1/1	473	1/1
2	523	60	105	1/1.25	523	1/1.25
3	573	75	88	1/1.5	573	1/1.5
4	623	90	74	1/1.75	623	1/1.75
5	673	105	63	1/2	673	1/2
6	723	120	44	1/2.25	723	1/2.25
Fixed conditions	1/1.5 *S*/*A*, − 105 µm		120 min, 723 K		120 min, − 74 µm	

shaking time, and organic-to-aqueous volume phase ratio were considered the main controlling extraction parameters.

All extraction experiments were performed in a 50-mL beaker at (25 ± 2) °C. The variable and fixed values for each studied parameter are represented in Table 2. After stirring the aqueous organic mixture, the phases were separated using a separating funnel, the aqueous raffinate phase was analyzed to identify the REEs, U, and Th concentrations, and the extraction efficiency was calculated according to the following Eq. 2.

$$\text{Extraction efficiency (\%)} = \left(\frac{C_o - C_e}{C_o}\right) \times 100 \quad (2)$$

where C_o and C_e were the original concentrations for REEs, Th, U, Ti, or Zr (mg/L) in the chloride feed solutions and their concentrations in the raffinate solutions after extraction (mg/L).

The stripping experiments of the loaded D2EHPA solvent were performed in a 50-mL glass beaker using a magnetic stirrer. To optimize the stripping process, several stripping factors were studied namely; the stripping solution type, the stirring time, and the phase ratio (VO/VA). By studying the variable factors under the fixed conditions as presented in Table 2, the mixture was settled down and the aqueous phase was separated using a separating funnel. The stripping efficiencies of the actinides were determined and calculated using Eq. 3.

$$\text{Stripping efficiency (\%)} = \left(\frac{C_S}{C_L}\right) \times 100 \quad (3)$$

where C_S and C_L were the concentrations of REEs, Th, U, Ti, or Zr (mg/L) in the stripping solutions after the stripping process and their original loaded concentrations on the solvent before extraction (mg/L).

2.6 Actinide Sediment Preparation

The stripping solutions containing the Th and U contents were subjected to complete precipitation of their actinide content. The pH of the stripping solutions was augmented to 2.2 using NaOH solution (50%), small portions of hydrogen peroxide (50%) were added, and the final pH was 2.0 [41, 42]. By allowing the slurry to sit for 6 h to attain complete precipitation, the produced precipitate was filtered, washed with H_2O_2 solution (2%) of the same pH, dried at 283 K for 6 h, and analyzed using SEM–EDX to identify the actinidepurity.

2.7 Rare Earth Sediment Preparation

The raffinate solutions, after removal of actinide contents using solvent extraction with D2EHPA, were collected and subjected to complete precipitation of the REE content using the oxalic acid method [43]. The raffinate solution pH was adjusted to pH 5 using sodium hydroxide solution (50%) additions, then the oxalic acid solution (10%) was added till the solution pH reached 1.0. The slurry was allowed to complete precipitation, settled, filtered, and washed with an oxalic acid solution (1%). The final sediment was dried, ignited at 1123 K, and analyzed using SEM–EDX to identify its constituents.

3 Results and Discussion

3.1 Mineralogical Investigation for Ras Baroud Polymetallic Concentrate

The pegmatite of the Ras Baroud area was previously discussed (Fawzy et al. 2020). The detailed mineralogical investigations of the studied samples revealed that the content of the light gangue silicate minerals (sp. gr. < 2.85) was 91.9% mass of the studied sample and represented as quartz

Table 2 Solvent extraction and stripping studied factors

	Parameters	Variable conditions	Fixed conditions
Solvent extraction process	D2EHPA concentration	0.075, 0.15, 0.225, 0.3, 0.45 mol/L	0.4 chloride Aqu. pH, 15 min stir. time, 1/2 *O*/*A* ratio
	Feed solution pH	0.2, 0.4, 0.6, 0.8	15 min stir. time, 0.3 mol/L solvent conc, 1/2 O/A ratio
	Stirring time	1, 3, 5, 10, 15 min	0.2 chloride Aqu. pH, 0.3 mol/L solvent conc, 1/2 *O*/*A* ratio
	Org/Aq phase ratio	1/6, 1/4, 1/2, 1/1, 2/1	0.2 chloride Aqu. pH, 0.3 mol/L solvent conc, 15 min stir. time
Stripping process	Stripping solution type	HCL, H_2SO_4, or HNO_3	4 mol/L acid conc, 10 min stir. time, 1/2 *A*/*O*
	Stripping acid Conc	1, 2, 3, 4, and 5 mol/L	Sulfuric acid Aqu phase, 10 min stir. time, 1/2 *A*/*O*
	Stirring time	1, 3, 5, 7, 10 min	4 mol/L sulfuric acid conc, 10 min stir. time, 1/2 *A*/*O*
	Aq/Org phases ratio	2/1, 1/1, 1/2, 1/3, 1/4	4 mol/L sulfuric acid conc, 10 min stir. time

and feldspar. On the other side, heavy minerals represent 7.9% mass which includes the existence of several economic and strategic minerals; Nb–Ta oxide minerals (euxenite (Y) and fergusonite (Y), REE minerals (xenotime (Y), monazite (Ce), allanite (Ce)), and thorium minerals (thorite and uranothorite). Thus, in addition to zircon and iron oxide minerals, muscovite represents about 5.3% mass (Figs. 1 and 2; Table 3).

The polymetallic concentrate was obtained from Ras Baroud pegmatite sample via successive physical beneficiation techniques that began with the comminution process, through crushing and grinding to prepare a feed material of about less than 1 mm, and then the comminuted raw material was subjected to a low-intensity magnetic separator for magnetite separation, followed by a separation of the paramagnetic minerals

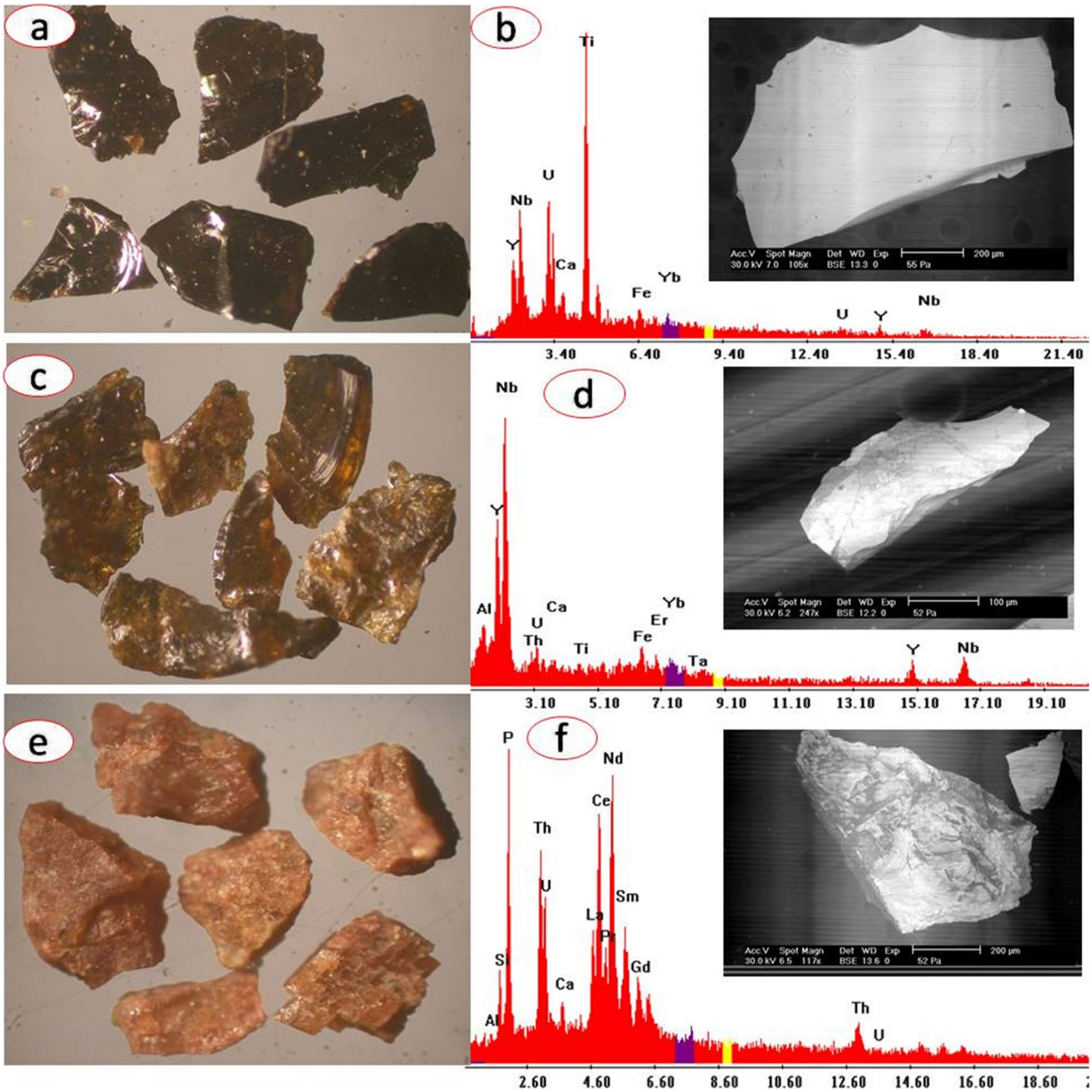

Fig. 1 Stereo microscopic image of euxenite-(Y) grains shows their optical properties (**a**); BSE images and EDX spectrum of euxenite-Y grains show their chemical composition (**b**); stereo microscopic image of fergusonite-(Y) grains shows their optical properties (**c**); BSE images and EDX spectrum of fergusonite-(Y) show their chemical composition (**d**); stereo microscopic image of monazite-(Ce) grains shows their optical properties (**e**); BSE images and EDX spectrum of monazite-(Ce) show their chemical composition (**f**)

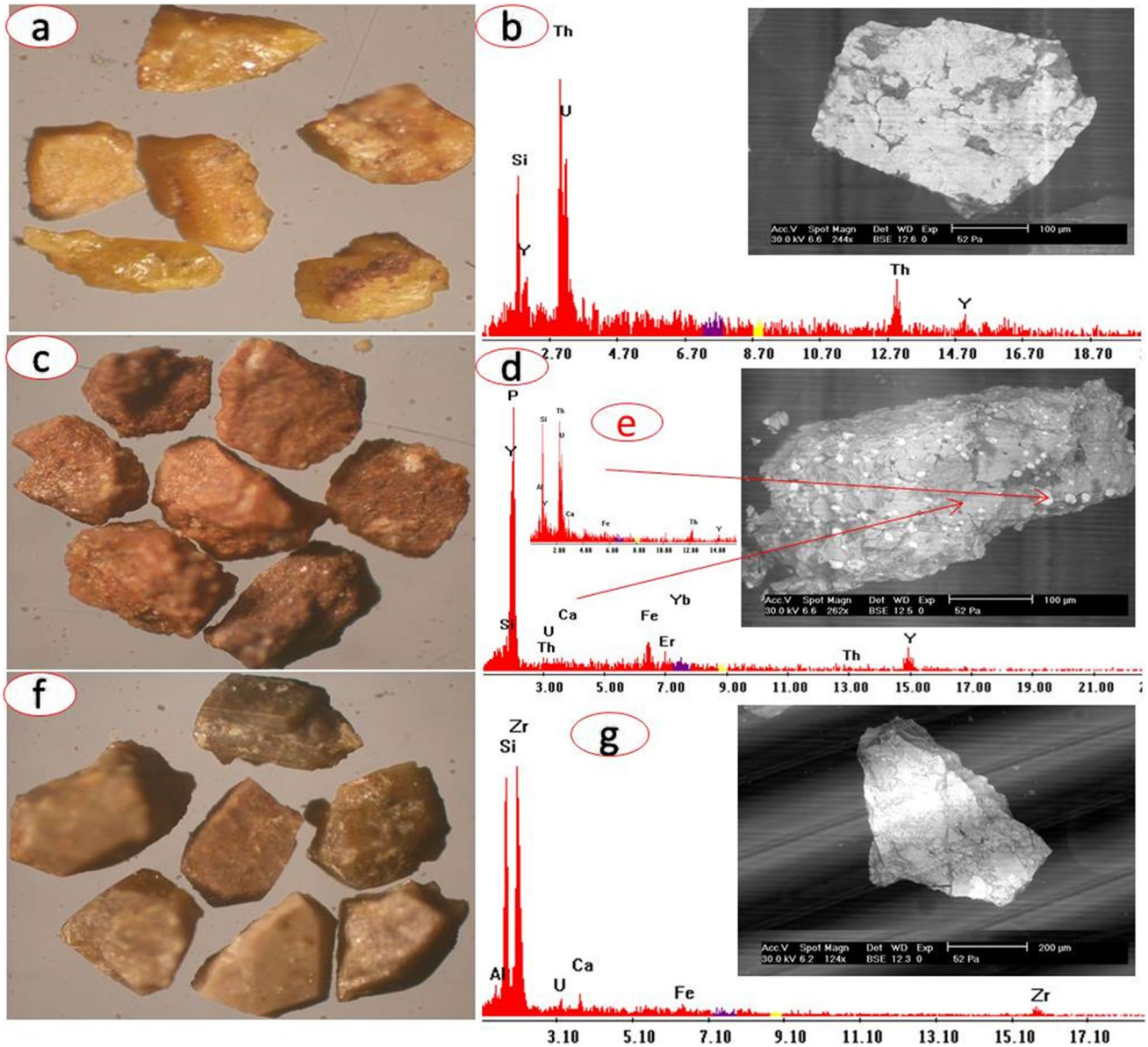

Fig. 2 Stereo microscopic image of uranothorite grains shows their optical properties (**a**); BSE images and EDX spectrum of uranothorite show its chemical composition (**b**); stereo microscopic image of xenotime-(Y) grains shows their optical properties (**c**); BSE images and EDX spectrum of xenotime-(Y) show its chemical composition (**d**); EDX spectrum of uranothorite inclusion inside xenotime grain show their chemical composition (**e**); stereo microscopic image of zircon grains shows their optical properties (**f**); BSE images and EDX spectrum of zircon show its chemical composition (**g**)

using a Carpco high-intensity magnetic separator. The non-magnetic fraction was used as a feed for the wet-gravity concentration process using the Wilfley shaking table (No. 13) to obtain a concentrate of zircon and reject the light gangue silicate minerals (quartz and feldspar).

Table 3 Mineralogical composition of the granitic pegmatite of Ras Baroud

Mineral	Quartz	Feldspar	Muscovite	Magnetite	Zircon
Weight %	28.7	63.2	5.3	0.58	0.58
Mineral	Xenotime-y, Monazite-Ce	Nb–Ta oxide minerals	Iron oxides	Thorite	Allanite-Ce
Weight %	0.62	0.51	0.06	0.33	0.12

The magnetic separation processes resulted in obtaining three products, which are as follows:

- Magnetite concentrate
- Paramagnetic mineral concentrate, which was obtained as a result of separating at 3 amperes magnetic field. This concentrate includes euxenite (Y), fergusonite (Y), xenotime (Y), monazite (Ce), allanite (Ce), thorite, uranothorite, iron oxides, and muscovite
- Quartz, feldspar, and zircon were obtained as a non-magnetic fraction at a magnetic field current of 3 amperes

To attain a clean zircon concentrate, the non-magnetic fractions were fed to the Wilfley shaking table. The obtained heavy fractions were mainly composed of zircon as well as fewer amounts of thorite, while the gangue light silicate minerals (quartz and feldspar) were discarded. Finally, a paramagnetic mineral concentrate with recovery efficiencies of 86.2, 96.6, and 91.2% for REEs, Th, and U elements, respectively, was obtained from the original sample as shown in Fig. 3.

Considerable contents of REEs, Th, U, Ti, and Zr were detected in the paramagnetic polymetallic concentrate using the EDX analysis as presented in Fig. 4. The illustrated SEM–EDX charts proved the presence of valuable minerals. These minerals were Monazite $(Ce,La,Th)PO_4$, Xenotime (Y) (Y(PO4)) Thorite $(Th,U)SiO_4$, Uranothorite $(Th,U)SiO_4$, Allanite (Ce) $((CaCe)(Al_2Fe^{2+})(Si_2O_7)(SiO_4)O(OH))$ euxenite $(Y,Ca,Ce,U,Th)(Nb,Ta,Ti)_2O_6$, and Zircon $Zr(SiO_4)$. Most of these minerals were refractory minerals and reflected the refractory nature of these polymetallic concentrates. So, aggressive opening conditions were needed

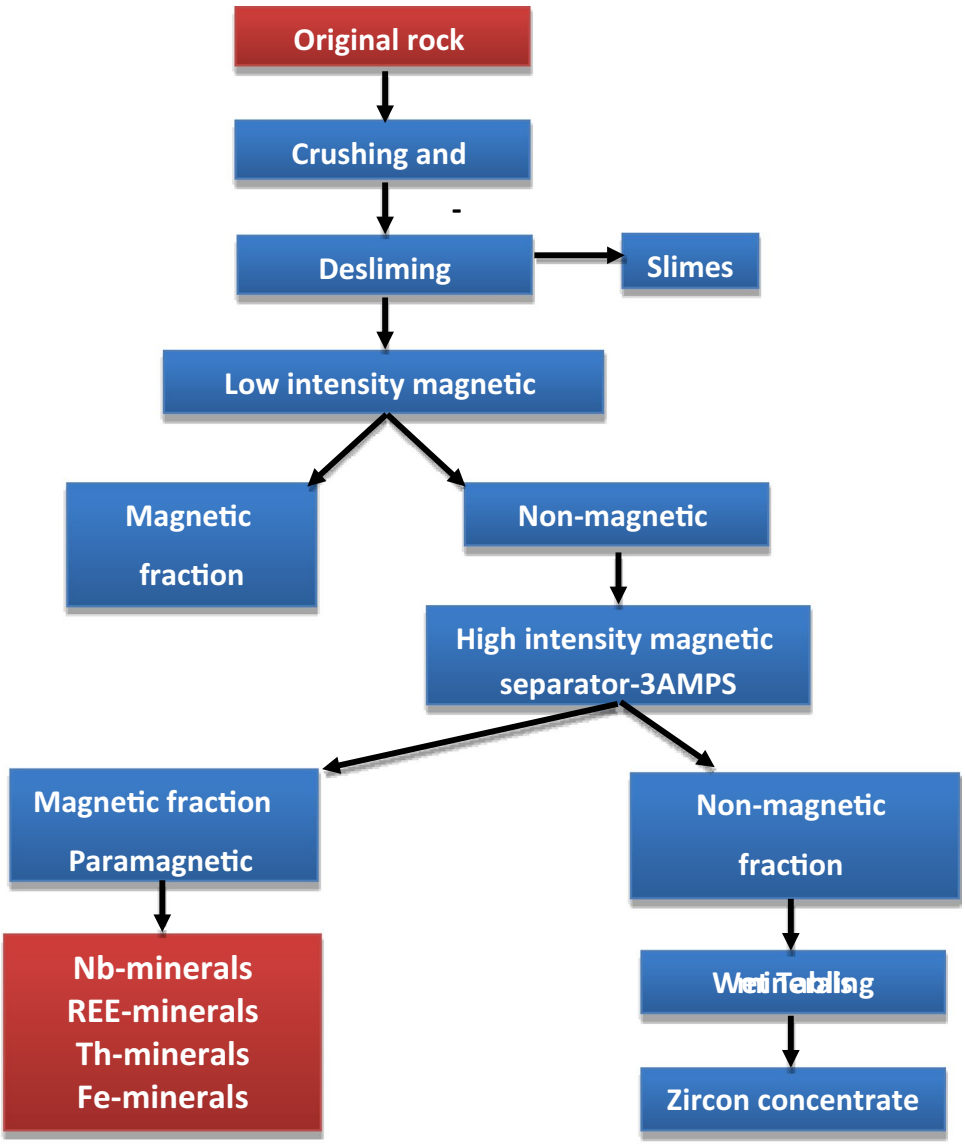

Fig. 3 A proposed flow-chart for obtaining polymetallic concentrate from pegmatite Ras Baroud

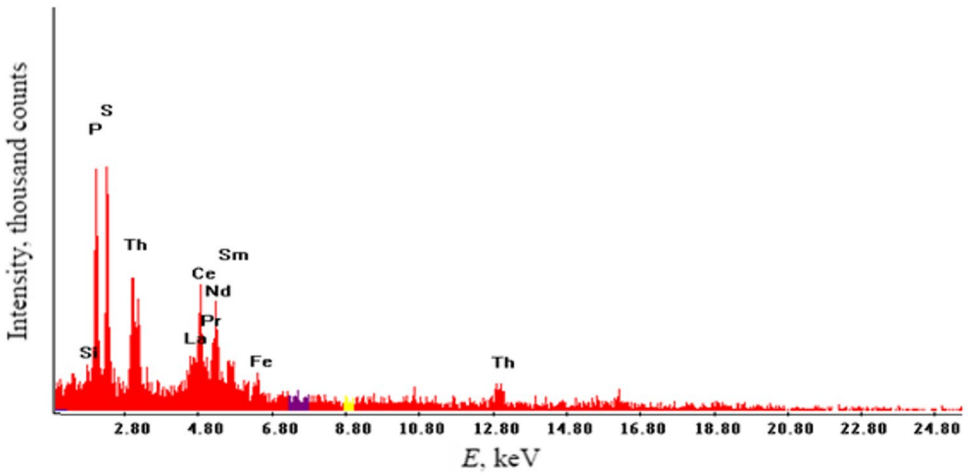

Fig. 4 EDX-spectrum for Ras Baroud polymetallic concentrate

to digest the concentrate and liberate the desirable elements from their crystal lattice.

3.2 Fusion Digestion Results

Three experimental groups were investigated using the CPD technique to study the dissolution behavior of REEs, Th, U, Ti, or Zr elements with alkaline digestion using sodium hydroxide as a flux. The essential target was to maximize the dissolution of REEs, U, and Th from their barren minerals (xenotime, monazite and allanite, thorite, and uranothorite minerals) while minimizing the dissolution of Zr and Ti contents (zircon and titanite). Eighteen fusion experiments were performed by varying the temperature versus fusion time, ore particle size versus solid-to-alkali (*S/A*) ratio, and fusion temperature versus solid to alkali ratio. The three binary groups and six experiments for each group were performed under certain fixed conditions as shown in Table 1.

From the dissolution results for REEs, Th, U, Ti, and Zr illustrated in Fig. 5, the following were noticed:

- From group 1 experiments, maximum dissolution for REEs, Th, and U was carried out using dissolution temperatures ranging from 673 to 723 K and dissolution times ranging from 105 to 120 min under a solid ore/alkali ratio of 1/1.5 and solid ore particle size of − 100 µm.
- From group 2 experiments, the solid ore/alkali ratio ranged from 1/1.5 and 1/2.25 with a solid ore particle size of − 74 µm could achieve maximum dissolution for desirable elements.
- From group 3 experiments, by varying the temperature and solid ore/alkali ratio together under fixing the time and the ore particle size (120 min, − 74 µm), from 623 to 723 K dissolution temperature with solid ore/alkali ratio ranging from 1/1.75 to 1/2.25 would achieve the maximum dissolution efficiencies for REEs, Th, and U.
- Using the maximum dissolution parameters of REEs, Th, and U elements, dissolution efficiency for Ti ranged from 40 to 60%. This may be attributed to the easy dissolution of allanite minerals with the difficult dissolution of titanite which contains the remaining Ti content under these conditions [43]. The dissolution results were paired with a minimum dissolution for Zr content under these moderate alkaline fusion digestions. Zircon and titanite minerals needed aggressive fusion digestion conditions with fusion temperatures over 923 K [23].
- From the results of the three groups, a significant increase in the digestion of the REEs, Th, U, Ti, and Zr elements was observed by studying the time versus temperature and *S/A* ratios versus the temperature, while by studying the *S/A* ratios versus the particle size, the change percentages in the REEs, Th, U, Ti, and Zr digestion were relatively small. So, the digestion parameters could be arranged according to their effect on the dissolution process as follows: digestion temperature > digestion time > *S/A* ratios > particle size.

3.3 Digestion Kinetics Results

A suggested model was utilized to explain the digestion chemical reactions of the mineral concentrate using sodium hydroxide as a fusing agent. The model namely shrinking core model was previously proved using mathematical treatments [23].

$$f\left(X_f, r\right) = (exp(-rR)).\left(\left(\frac{1}{K_D}\right)[1 - 3(1 - X_f)^{\frac{2}{3}} + 2(1 - X_f)] + \left(\frac{1}{K_C}\right)[1 - \left(1 - X_f\right)^{\frac{1}{3}}]\right) \quad (4)$$

Shrinking Core Model Equation (Eq. 4)

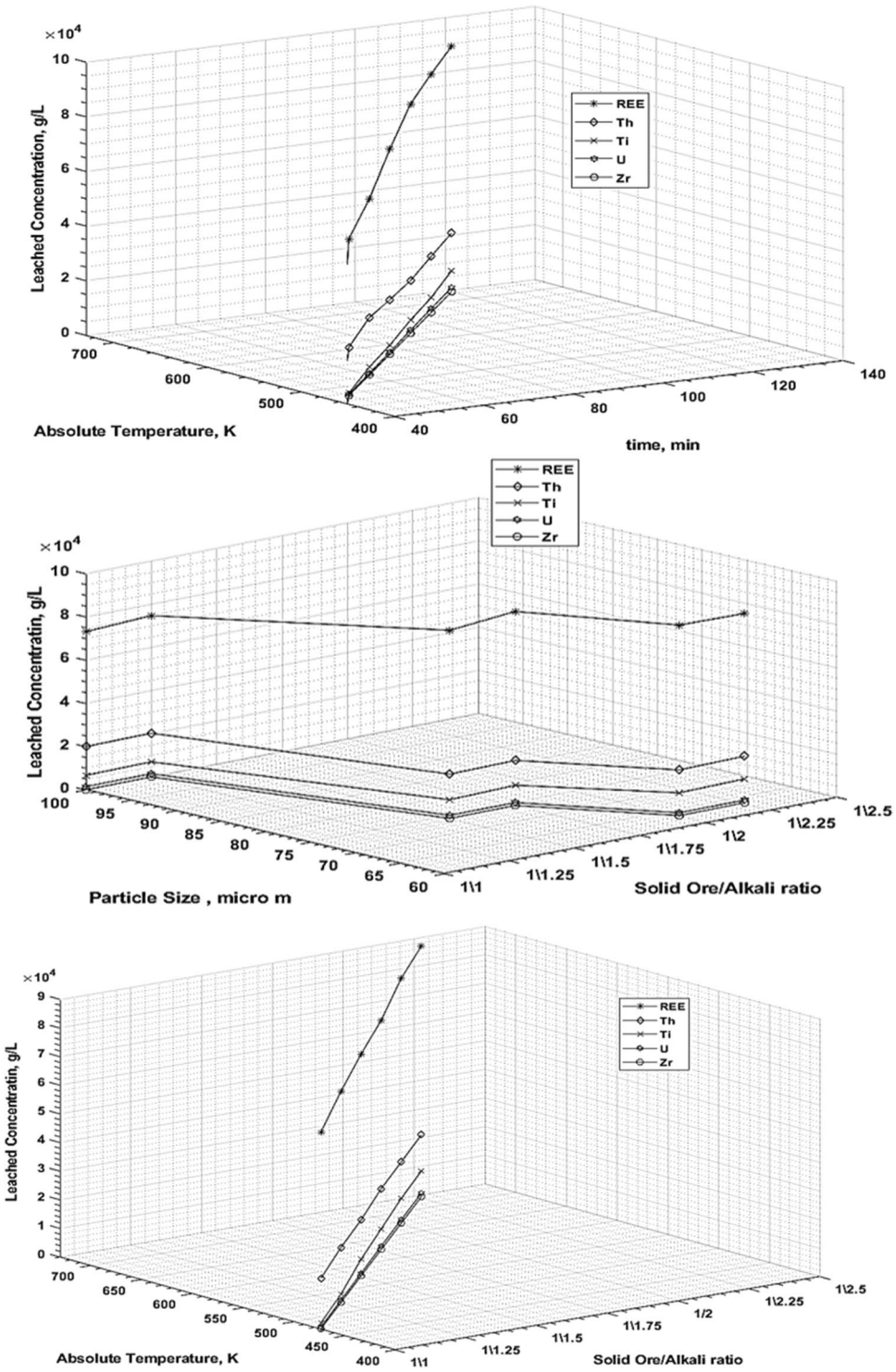

Fig. 5 The studied fusion digestion groups using CPD technique for Ras Baroud mineral concentrate

where the terms r and R represent the solid-to-alkali (S/A) ratios and the molar gas constant. The terms X_f, k_D, and k_C represent the resistances to the fractional conversion external mass transfer, product layer diffusion, and chemical reaction, respectively.

By applying the suggested model equation to the results obtained from the three digestion groups, the resulting kinetic parameters for the digestion processes of REEs, Th, U, Ti, and Zr elements were graphed using the MATLAB program in three-dimensional 3D curves, as shown in Figs. 6

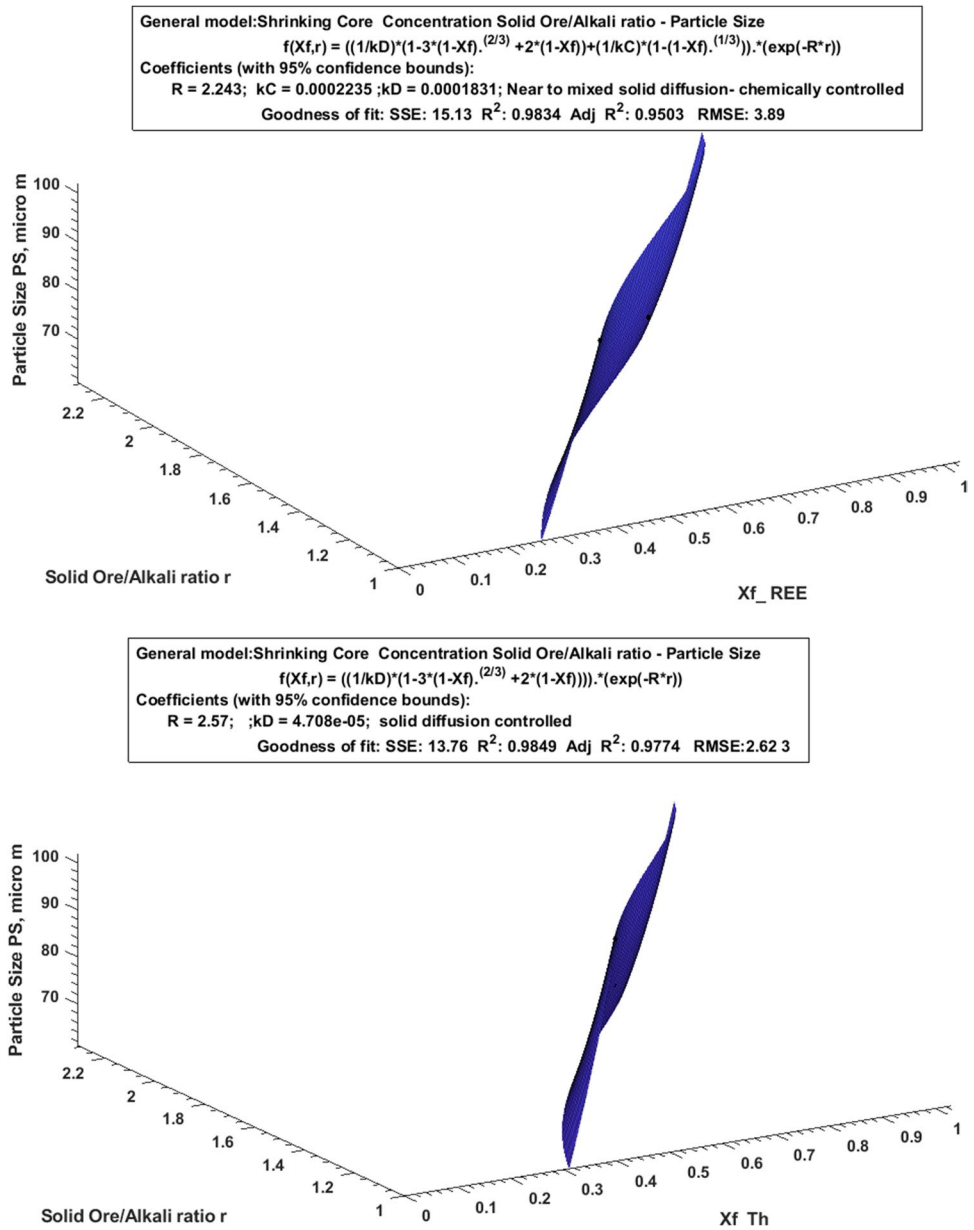

Fig. 6 Shrinking core model surfaces for digestion processes of REEs, Th, and Ti

and 7. The R^2, X_f, k_D, and k_C values for the digestion processes using NaOH were illustrated in Table 4.

The shrinking core model assumes the particles are uniform non-porous grains. Initially, the reaction occurs on the grain surface, and then the reaction zone moves into the solid leaving a product layer behind. The total radius of the particle remains constant, while the radius of the unreacted core and the layer of products vary over time as a function of conversion. The approximate solution of the shrinking core model applied in this work was a combination of the resistances that can simultaneously occur in a particle under reaction: alkali diffusion in the layer surrounding the particle, alkali diffusion through the product layer around the unreacted core, and chemical reaction on the unreacted core surface. Introducing Arrhenius relation in the graphical simulation that relates the conversion as a function of solid ore to alkali ratio for a spherical particle is given by Eq. 5.

From the experimental results graphed in Figs. 6 and 7 and illustrated in Table 4, the shrinking core results using group 1 and 3 experiments indicated that the interaction between the alkali and the ore was carried out through a mix of solid diffusion and chemical control. On the other side, from group 2 results for the digestion processes of REEs, Th, U, Ti, and Zr elements, which have the minimum value for KD ($k_D < k_C < X_f$), the interaction between the alkali and the ore was performed through a solid diffusion control.

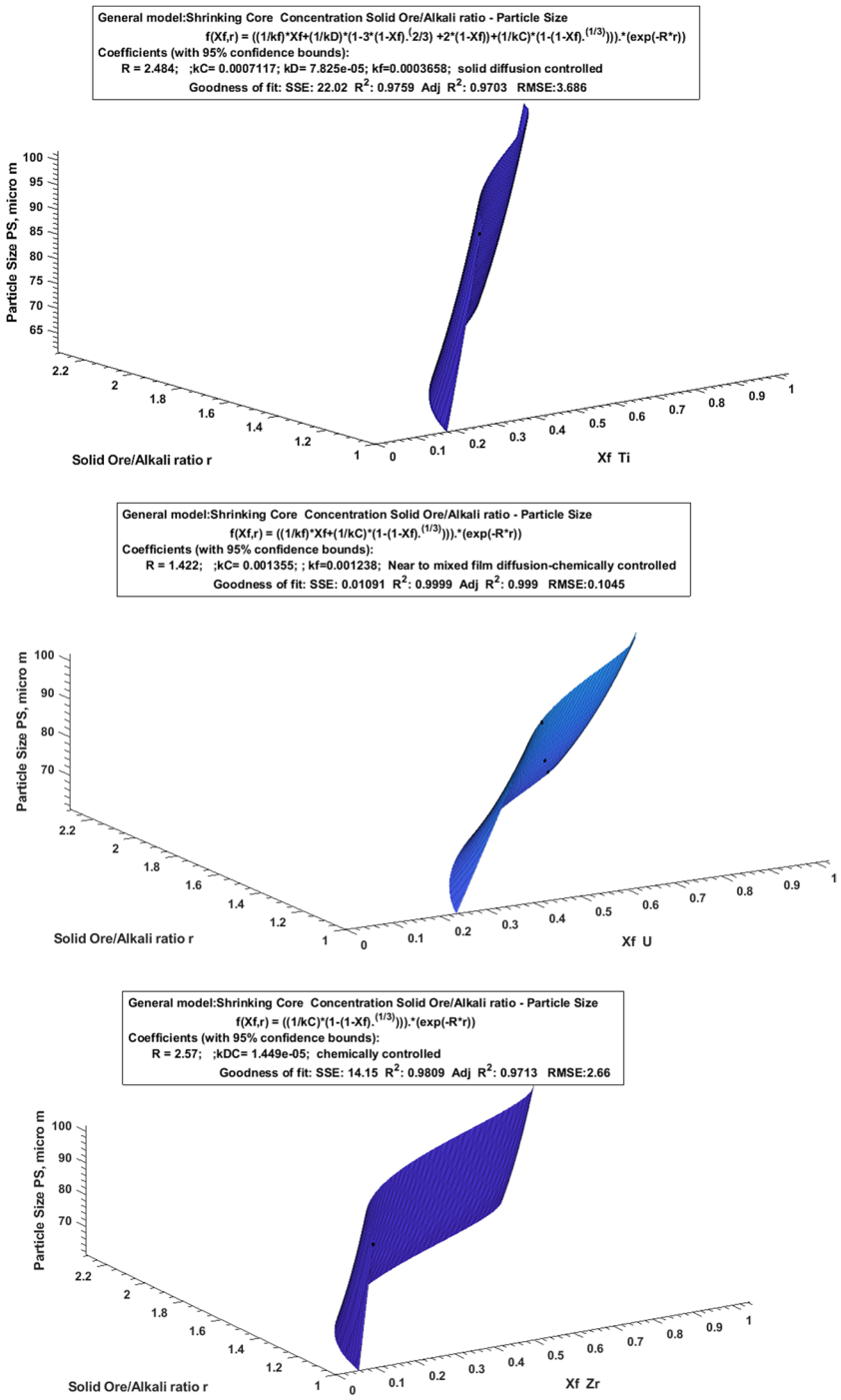

Fig. 7 Shrinking core model surfaces for digestion processes of U, and Zr

3.4 Digestion Thermodynamics Results

By applying the fusion digestion results obtained from group 3 using the CPD technique, a binary study between varied temperatures and solid ore to alkali ratios was performed to determine the thermodynamics of REEs, Th, U, Ti, and Zr. Temperatures from 473 to 723 K and ratios from 1/1 to 1/2.25 *S/A* were performed under fixed conditions. The thermodynamic parameters of the digestion process using NaOH were determined using two models' equations, namely Equilibrium Constant-Van't Hoff model equation (Eq. 5) and Floatotherm including Van't Hoff model equation (Eq. 6). The two equations were previously proven [22, 23]. Two types of equations were utilized in

Table 4 The three groups' digestion parameters using shrinking core model with mathematical analysis

Groups		REE	Th	U	Ti	Zr
1	X_f	0.009838	0.010387	0.00842	0.006976	0.008878
	K_d	0.007079	0.00789	0.005596	0.003908	0.005371
	K_c	0.007014	0.007571	0.005874	0.004571	0.005819
2	X_f	0.008004	0.00801	0.008123	0.006771	0.005109
	K_d	0.004002	0.003838	0.003945	0.00316	0.002437
	K_c	0.004691	0.004611	0.004695	0.00393	0.003087
3	X_f	0.416007	0.425349	0.388443	0.355422	0.363831
	K_d	0.24214	0.251574	0.229686	0.213764	0.207283
	K_c	0.270378	0.277585	0.256336	0.23895	0.238371

the determination of the thermodynamic parameters, the distribution coefficient k_d and the uptake q_m, respectively.

$$f(t,T) = (t^n).exp\left(\left(\frac{-1000\Delta H}{RT}\right) - \frac{\Delta S}{R}\right) \tag{5}$$

$$f(T,C) = \frac{\left((q_m - q_e).\left(exp\left(\left(\frac{-1000\Delta H}{RT}\right) - \frac{\Delta S}{R}\right)\right).C^m\right)}{\left(1 + \left(exp\left(\left(\frac{-1000\Delta H}{RT}\right) - \frac{\Delta S}{R}\right)\right).C^n\right)^g} \tag{6}$$

where q_e and q_m were the maximum uptake that can be liberated by these matrices (system conditions) and the maximum uptake that ore can give, respectively. Practically, n, m, and g were the powers to be estimated that indicate the effect of their variables at which the highest value indicated the greatest effect on the reaction. K_d (ml/g), ΔH (KJ/mol), ΔS (J/mol·K), t (min), T (Kelvin), and R (KJ/K·mol) were the distribution coefficient, the enthalpy, the entropy, the digestion time, the temperature in Kelvin, and the molar gas constant, respectively. The Gibbs free energy, ΔG (KJ/mol), was calculated from the following equation (Eq. 7).

$$\Delta G = \Delta H - T\Delta S \tag{7}$$

The two suggested models were represented in 3D using MATLAB as shown in Figs. 8, 9, 10, and 11. The thermodynamic parameters, namely, enthalpy, entropy, Gibbs free energy, and the correlation coefficient for REEs, Th, U, Ti, and Zr using the two models are collected in Table 5. It was indicated from the results of the thermodynamic parameters that the endothermic nature of the digestion processes of REEs, Th, U, Ti, and Zr using sodium hydroxides was proven from the positive value of ΔH. Therefore, all reactions were temperature-dependent. The positive values of ΔS for all digestion reactions were confirmed which indicates an increase in the randomness at the solid/solution interface during the attack of fused alkali on the ore particles. All digestion reactions have a feasible and spontaneous nature due to the negative value of ΔG.

3.5 Solvent Extraction Results

3.5.1 Feed Solution Preparation

By applying the optimal digestion parameters to Ras Baroud polymetallic concentrates and washing the fused cake several times with DDW, several acids, namely, hydrochloric, sulfuric, nitric, and citric acids, were examined to determine the optimal acid that has maximum leaching efficiency for REEs, Th, and U contents. From the obtained data illustrated in Fig. 12, the hydrochloric acid of 2 mol/L has a maximum leaching efficiency for the REEs, Th, and U desirable elements under experimental conditions of solid to the acid solution of 1/10, dissolution temperature of 253 K, and stirring for 60 min. Approximately, all REEs, Th, and U contents were dissolved in the hydrochloric acid solution forming a chloride feed solution which has been used in the subsequent separation stages.

3.5.2 Batch Extraction Results

A series of recovery experiments were performed using varied conditions values, namely, from 0.075 to 0.45 mol/L D2EHPA solvent concentrations, from 0.2 to 0.8 pH of the feed solution, from 1 to 15 min stirring time, and from 1:6 to 2:1 *O*/*A* ratios. These variations were performed under fixed conditions as mentioned in Table 2. Kerosene was the preferred choice to be used as diluent which was considered economical and had other advantages during the extraction process as previously mentioned [43]. The chloride feed solutions containing REEs, Th, and U ions were subjected to a solvent extraction stage to separate and remove the radioactive actinide content from the REEs and produce a pure REEs oxide cake from the Ras Baroud polymetallic concentrate.

From the recovery results illustrated in Fig. 13a, the solvent concentration of 0.3 mol/L of D2EHPA dissolved in kerosene as a diluent was the optimal solvent concentration. About 97.5 and 92.6% extraction

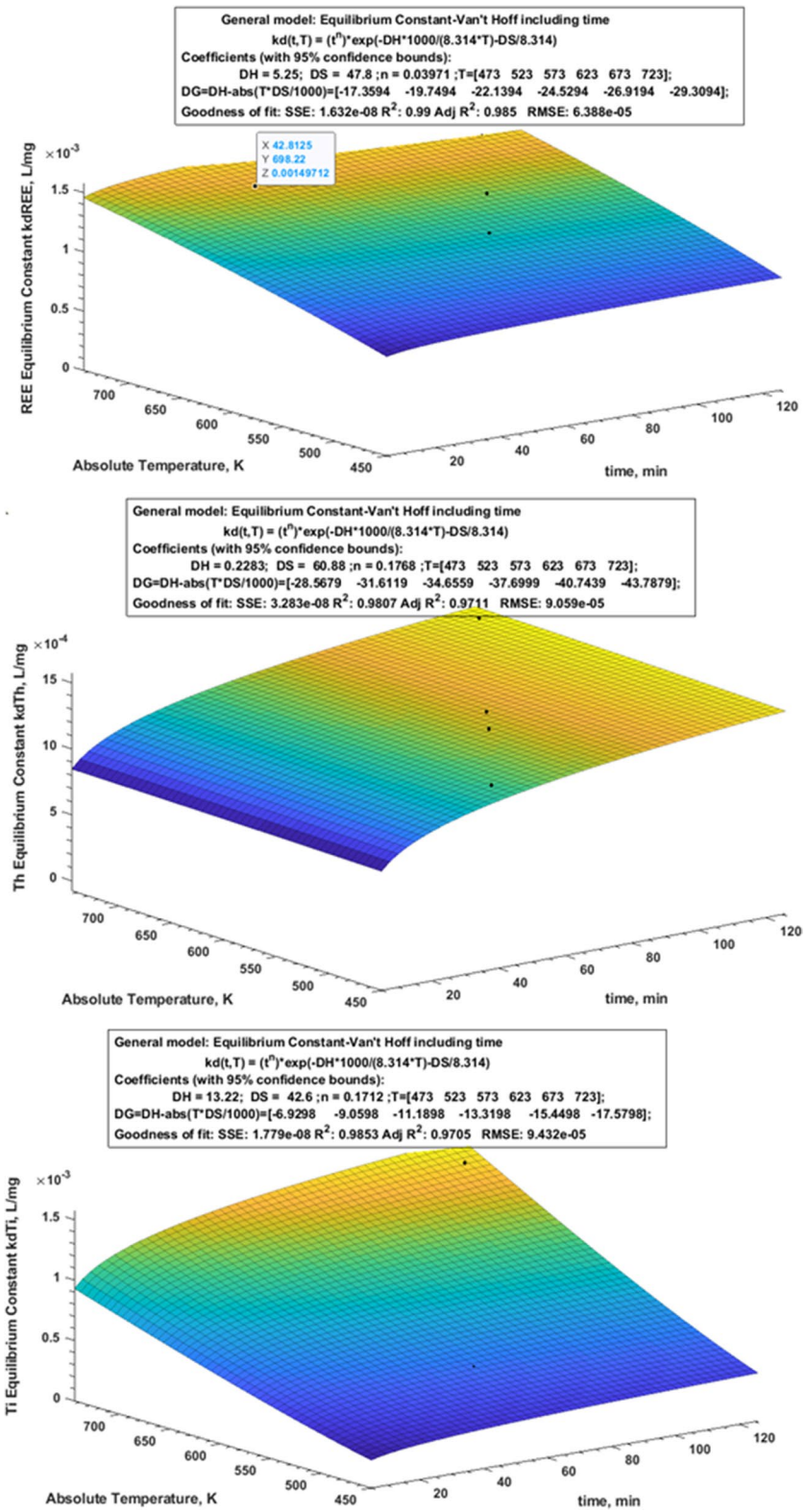

Fig. 8 Equilibrium constant-Van't Hoff model curves for REEs, Th, and Ti

efficiencies for Th and U were achieved; this was combined with about 4.8% extraction efficiency for REEs which was considered the lowest REE extraction efficiency. By increasing the solvent concentration, the recovery efficiency of REEs was sharply increased with simple enhancements in Th and U cases. So, 0.3 mol/L D2EHPA was considered the best choice to perform the next parameter steps.

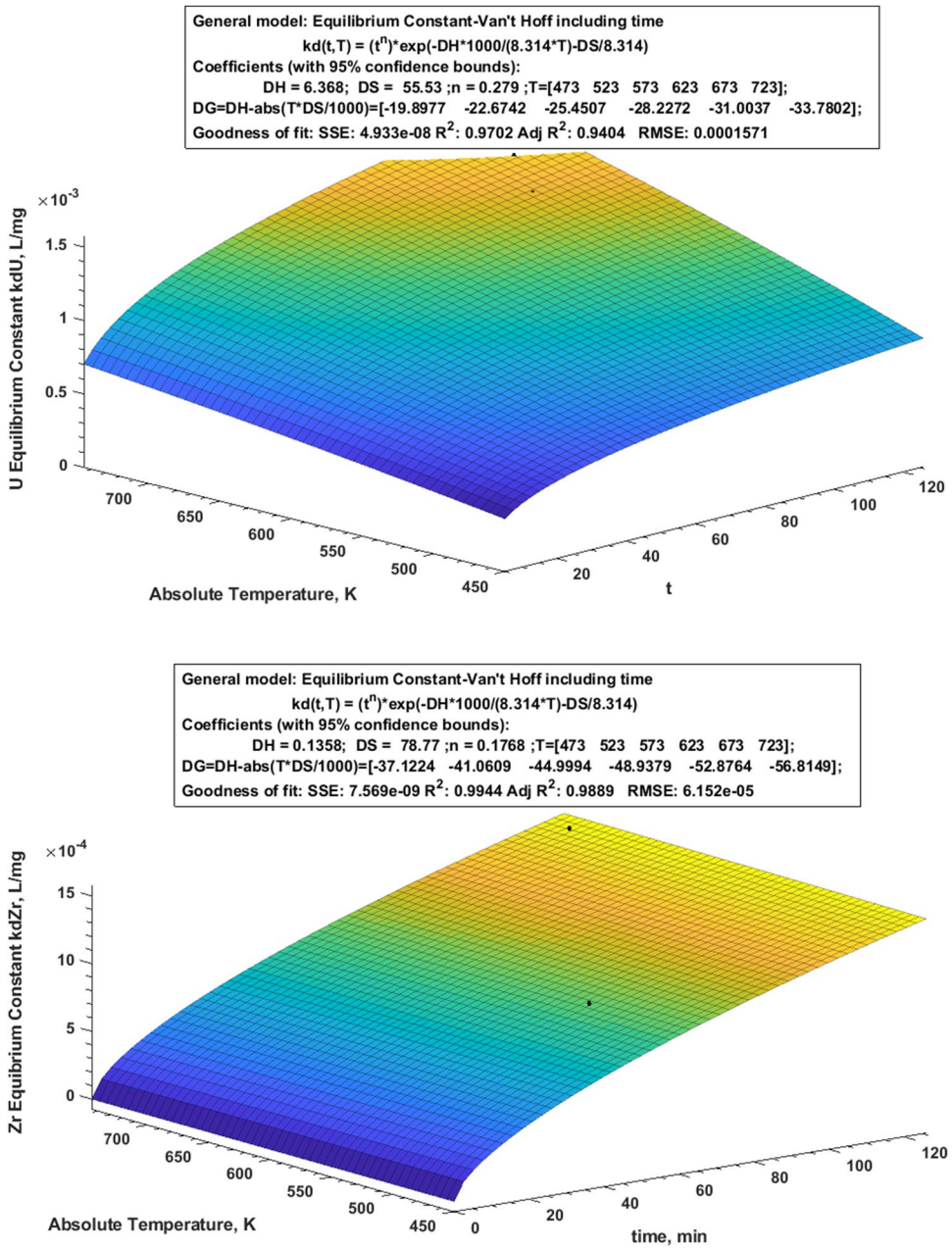

Fig. 9 Equilibrium constant-Van't Hoff model curves for U and Zr

A wide range for the chloride feed solution was examined to determine the optimal pH as shown in Fig. 13b. To increase the extraction of Th and U and retain the raffinate-contained REE content after the extraction process, low values of pH (0.2–0.4) were preferred that succeeded in a complete recovery for actinide contents and remaining a raffinate solution contained about 95% of REE content. So, the pH of 0.2 was considered the best feed solution pH to perform the recovery processes.

The reaction time was considered one of the most important factors to study at which the equilibrium time of the chemical reaction could be determined. The stirring time range was studied from 1 to 15 min under fixed conditions, namely, 0.3 mol/L D2EHPA concentration, 0.2 feed solution pH, and 1/2 *O*/*A* ratio. From the illustrated Fig. 13c, the optimal stirring time between the chloride solution and the D2EHPA solvent was 15 min at which a complete removal of the actinidecontent from the chloride solution and keeping all REE content in the raffinate solution was achieved. This was considered the solvent extraction main target.

The actinide (Th and U) recovery from the chloride solution using D2EHPA solvent was investigated using various *O*/*A* ratios ranging from 1/6 to 2/1. As shown in Fig. 13d, complete removal of actinides was carried

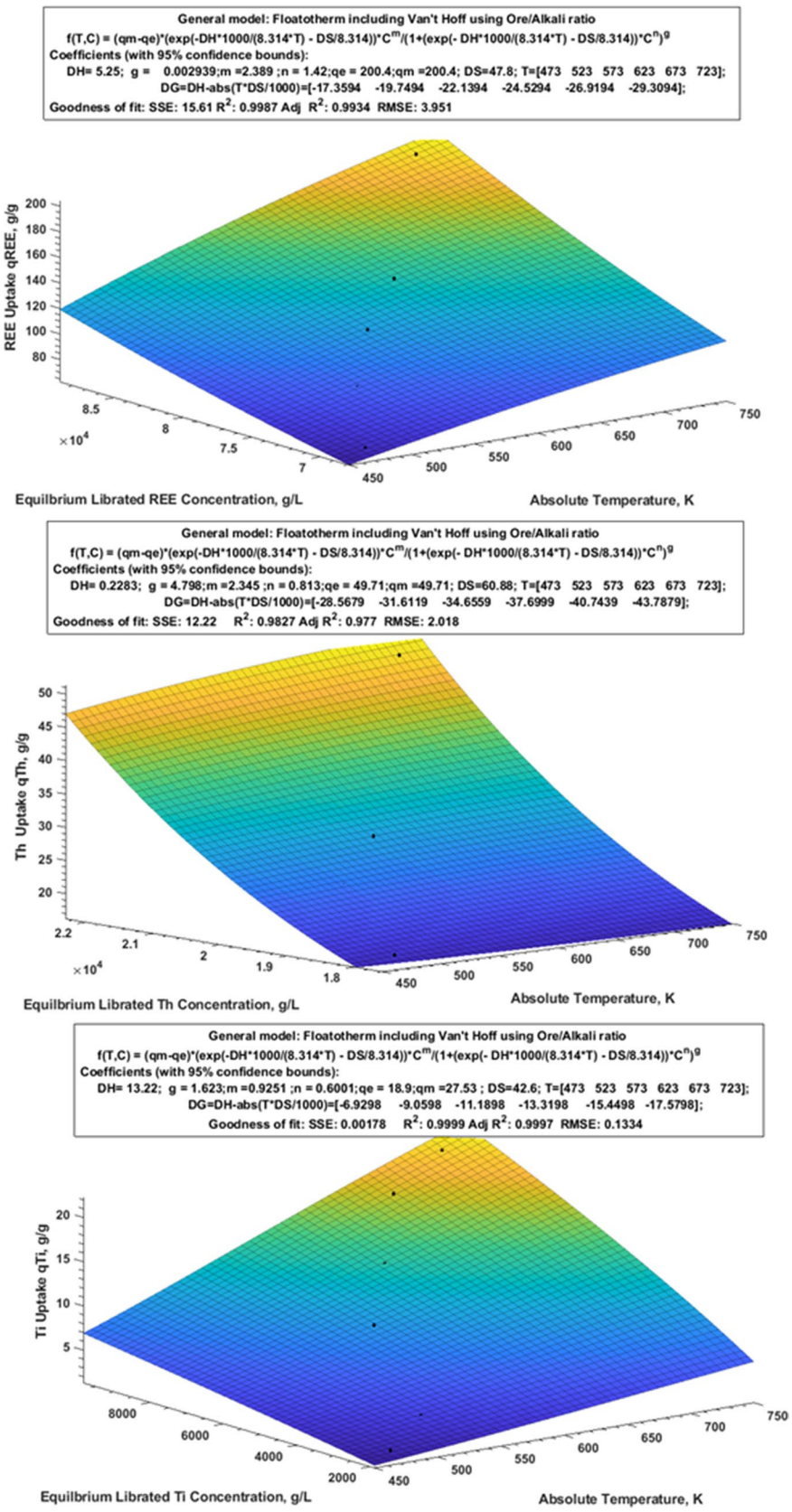

Fig. 10 Floatotherm including Van't Hoff model curves for REEs, Th, and Ti

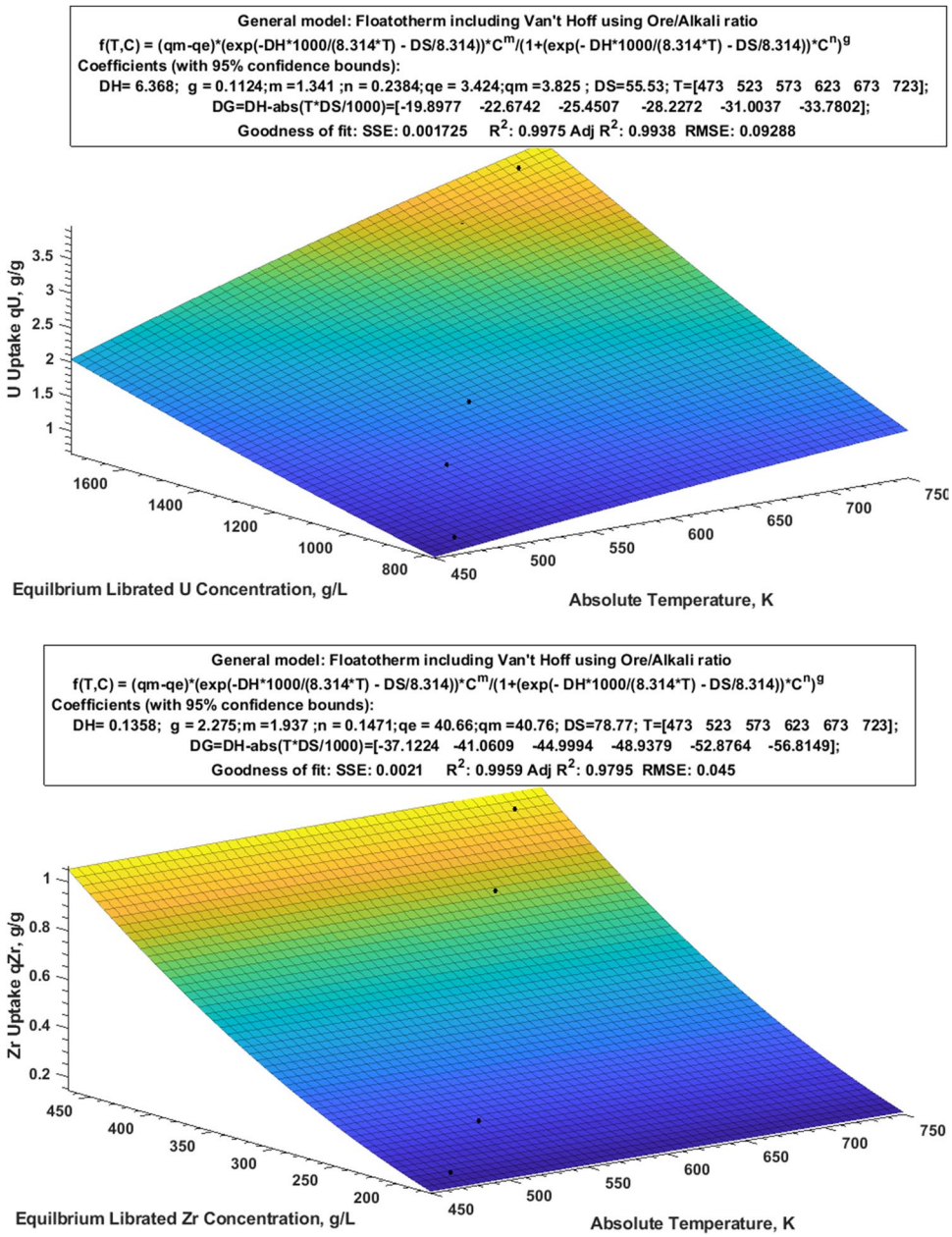

Fig. 11 Floatotherm including Van't Hoff model curves for U and Zr

Table 5 Thermodynamics parameters for REEs, Th, U, Ti, and Zr digestion processes

Model	Element	q_e	q_m	ΔH	ΔS	ΔG, K						R^2
						473	523	573	623	673	723	
Equilibrium Constant-Van't Hoff	REE	–	–	5.3	47.8	−17. 4	−19.8	−22.1	−24.5	−26.9	−29.3	0.990
	Th	–	–	0.2	60.9	−28.6	−31.6	−34.7	−37.7	−40.7	−43.8	0.981
	U	–	–	6.368	55.53	−19.9	−22.7	−25.5	−28.2	−31.0	−33.8	0.970
	Ti	–	–	13.2	42.6	−6.9	−9.1	−11.2	−13.3	−15.5	−17.6	0.985
	Zr	–	–	0.1	78.8	−37.1	−41.1	−44.9	−48.9	−52.9	−56.8	0.994
Floatotherm including Van't Hoff	REE	200.4	200.4	5.3	47.8	−17.4	−19.8	−22.1	−24.5	−26.9	−29.3	0.999
	Th	49.7	49.7	0.2	60.9	−28.6	−31.6	−34.7	−37.7	−40.7	−43.8	0.983
	U	3.4	3.8	6.4	55.5	−19.9	−22.7	−25.5	−28.2	−31.0	−33.8	0.998
	Ti	18.9	27.5	13.2	42.6	−6.9	−9.1	−11.2	−13.3	−15.5	−17.6	0.999
	Zr	40.66	40.76	0.1	78.8	−37.1	−41.1	−44.9	−48.9	−52.9	−56.8	0.996

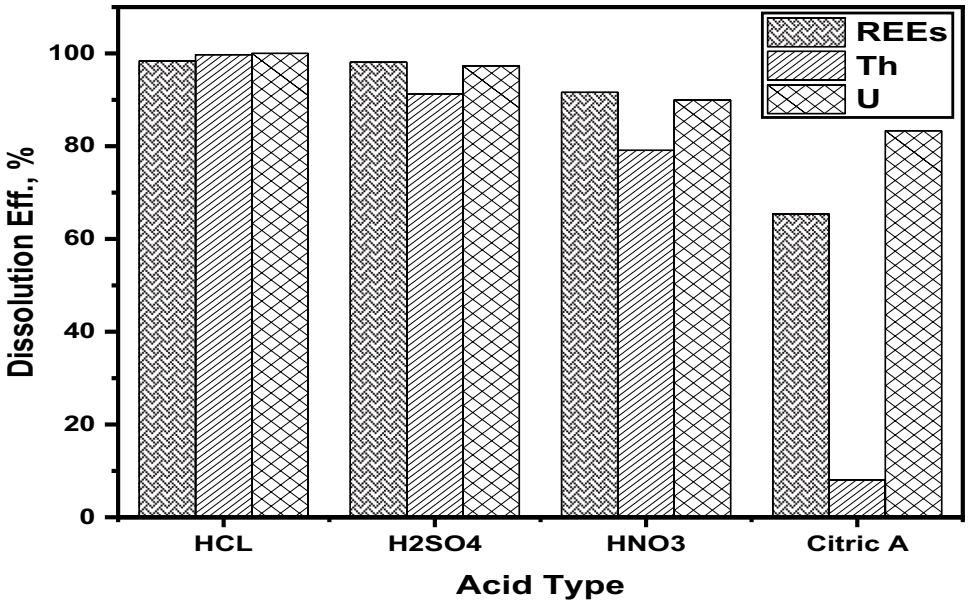

Fig. 12 Dissolution efficiencies for REEs, Th, and U using different acids

out in one contact using *O/A* ratios of 2/1, 1/1, and 1/2. However, using a high aqueous to solvent of 1/6 *O/A* ratio resulted in enhancing the actinide uptake and producing a raffinate containing all the REE content with small portions from Th and U which needed further treatments to be removed.

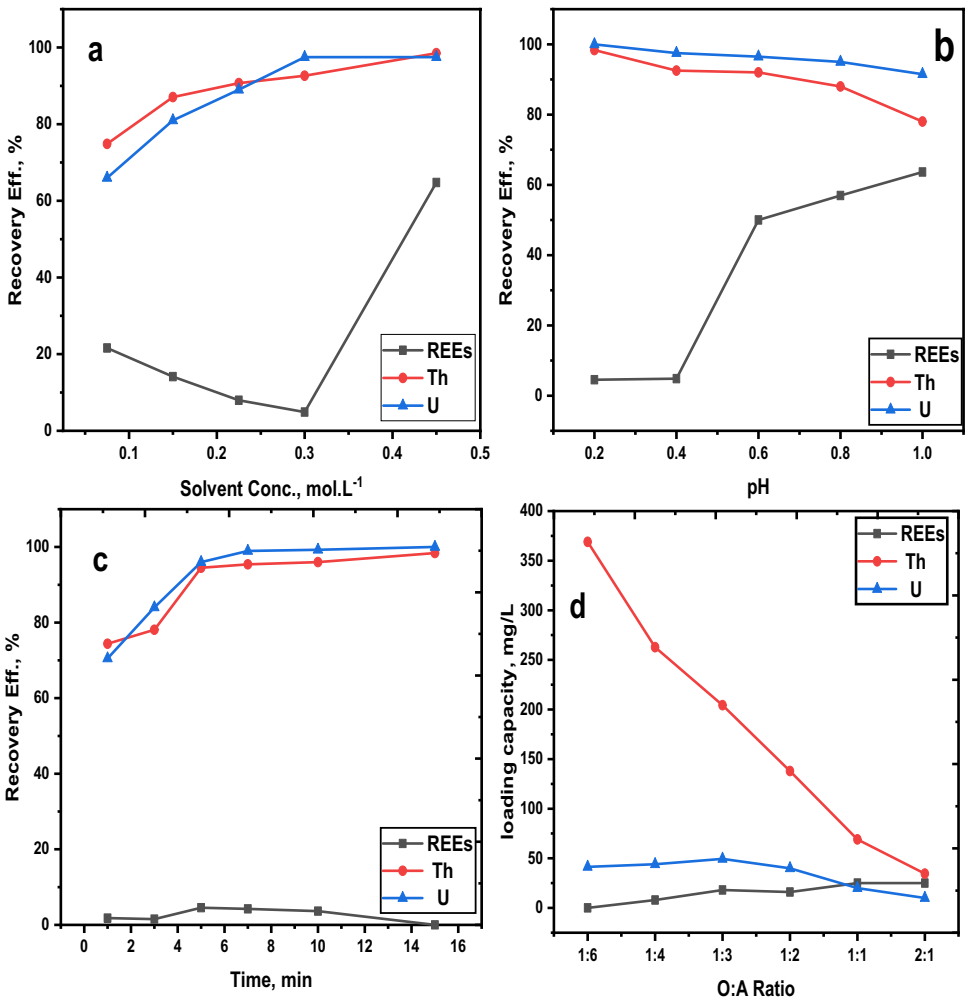

Fig. 13 Solvent Extractions factors for REEs, Th, and U on D2EHPA solvent

3.5.3 Stripping Results

To back-extract Th and U ions from the D2EHPA loaded organic phase, stripping tests were investigated to determine the confident stripping agent and the other relevant stripping parameters namely acid concentration, stirring time, and *A*/*O* ratio. All the stripping processes were performed using a 400-rpm stirring rate and at room temperature (25 ± 2).

To recover the loaded Th and U from the loaded D2EHPA, hydrochloric, nitric, sulfuric, and citric acids were tested as stripping agents for the loaded actinides in the studied solvent. Each acid of 4 mol/L concentration was contacted with the loaded organic phase with an aqueous-to-organic ratio of 2/1 and stirred for 15 min. The plotted figure (Fig. 14a) indicated that sulfuric acid was the optimal stripping acid compared with the other acids. The other studied acids failed in the re-extraction of the Th and U contents from the loaded solvent. So, the subsequent stripping processes were carried out using sulfuric acid as a stripping agent.

Different concentrations of sulfuric acid were tested to determine the optimal acid concentration causing maximum recovery for the actinide contents. From 1 to 5 mol/L, sulfuric acid concentrations as an aqueous phase were studied under fixed conditions of 2/1 *A*/*O* ratio and 15 min of stirring. From the results plotted in Fig. 14b, 2.5 mol/L sulfuric acid concentration was the preferable aqueous acid concentration resulting in maximum stripping for both Th and U from the loaded solvent. By increasing the acid concentration over 2.5, sharp decreases in the U stripping efficiencies were detected. So, 2.5 mol/L sulfuric acid was the choice to perform the stripping processes.

The influence of stirring time on the stripping efficiency of actinides was investigated using a 2.5 mol/L sulfuric acid concentration aqueous solution and a 2/1 *A*/*O* ratio. Varied stirring times from 1 to 20 min were studied to determine the equilibrium time. Maximum stripping efficiency for both Th and U was achieved after prolonging the stirring time for the stripping process by 20 min. So, as shown in Fig. 14c, the stirring time of 20 min was the optimum stripping time for both Th and U.

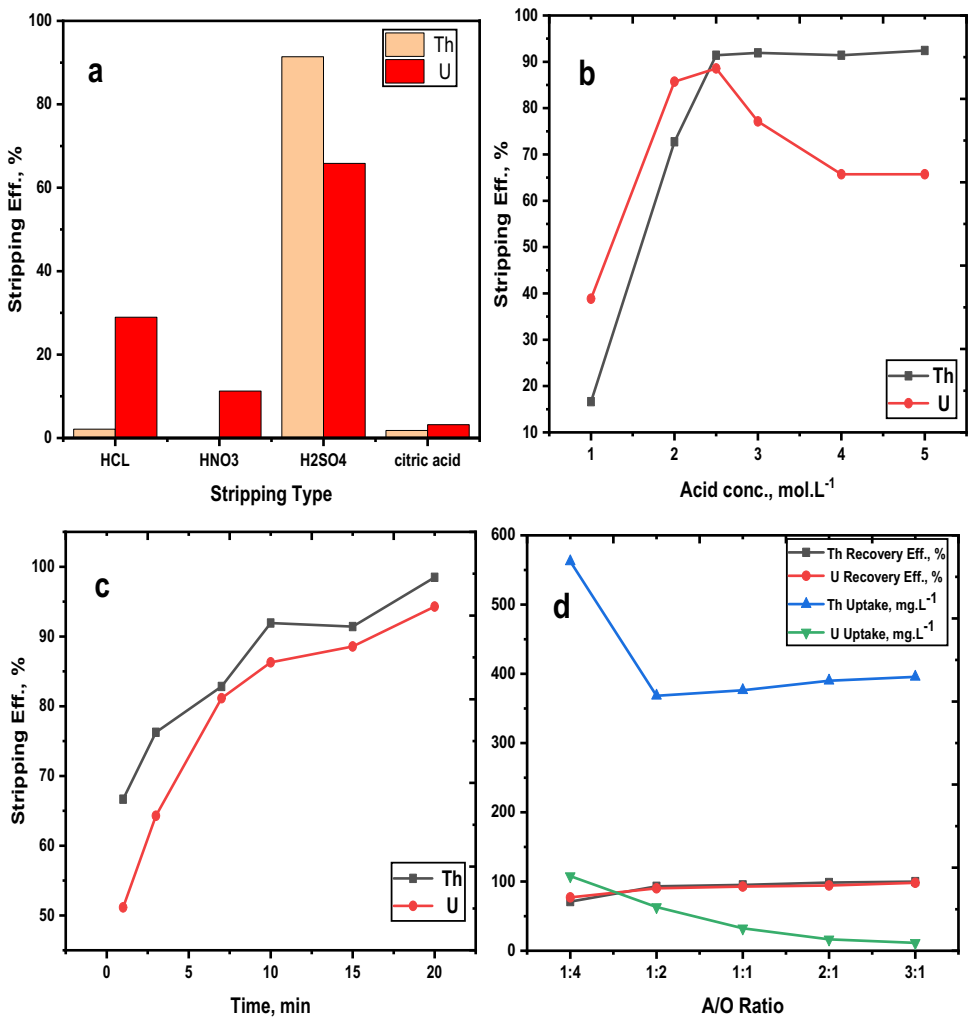

Fig. 14 Stripping factors for Th and U from loaded D2EHPA

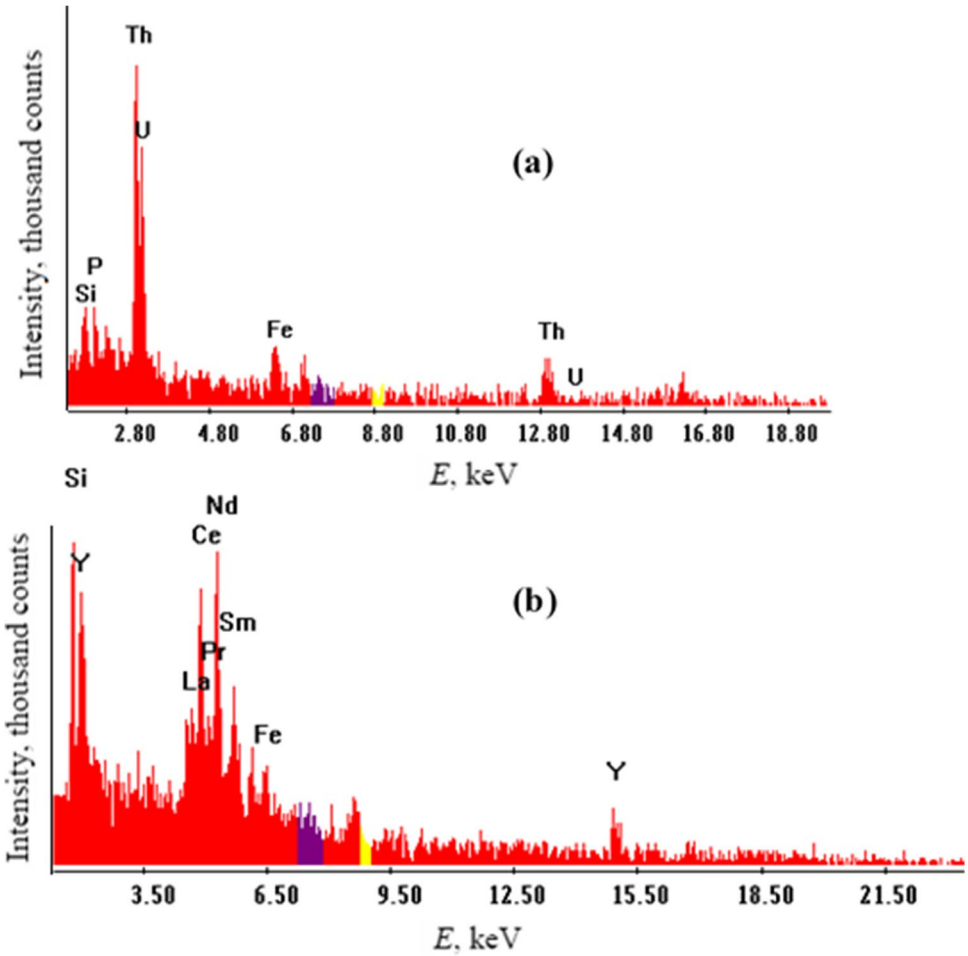

Fig. 15 EDX-charts for final REEs product (**a**) and Th and U cake (**b**)

The effect of phase ratio was studied using different phase ratios ranging from 1/4 to 3/1 *A*/*O*. The fixed conditions were 20 min of stirring time and 2.5 mol/L sulfuric acid concentration aqueous solutions. From the obtained results plotted in Fig. 14d, a sharp increase in the Th and U recovery was carried out using ratios of higher organic than aqueous phase as 1/3 and 1/4 *A*/*O*, this was combined with small decreases in the stripping efficiencies of Th and U, and this was attributed to the dilution factor. So, the stripping processes were preferably performed using equivolume from the organic and aqueous phases (*A*/*O* of 1/1) at which all the actinides were extracted from the loaded solvent in one stage.

3.6 Rare Earths and Actinide Sediment Preparation Results

A series of recovery experiments were performed to precipitate the REEs, Th, and U contents. Previously, the Th and U contents were separated together using D2EHPA organic solvent from the chloride feed solution of the Ras Baroud mineralization. The actinide contents were successfully re-extracted using sulfuric acid. The precipitation of the Th and U contents was investigated by enhancing the pH to 2.0 using a sodium hydroxide solution of 50%. The prepared precipitate was dried and analyzed to identify its constituents. From the resulting EDX chart plotted in Fig. 15a, a produced cake with significant Th and U contents was attained from the studied mineralization.

On the other side, the raffinate solution after the solvent extraction stage was recycled to recover the REE content. Small portions of 10% oxalic acid were added to the raffinate solution after adjusting its pH to 5 using 50% sodium hydroxide solution; then the oxalic acid solution (10%) was added till the solution pH reached 1.0. After settling and filtration, the filtrated cake was washed with 1% oxalic acid solution several times to remove the undesirable gangues, dried at 383 K for 6 h, ignited at 1123 K, and finally analyzed to identify its constituents. From the resulting EDX chart plotted in Fig. 15b, a finally produced REE cake was obtained with about 90% REE concentrations. There was not any appearance for Th and U in the EDX-chart of the

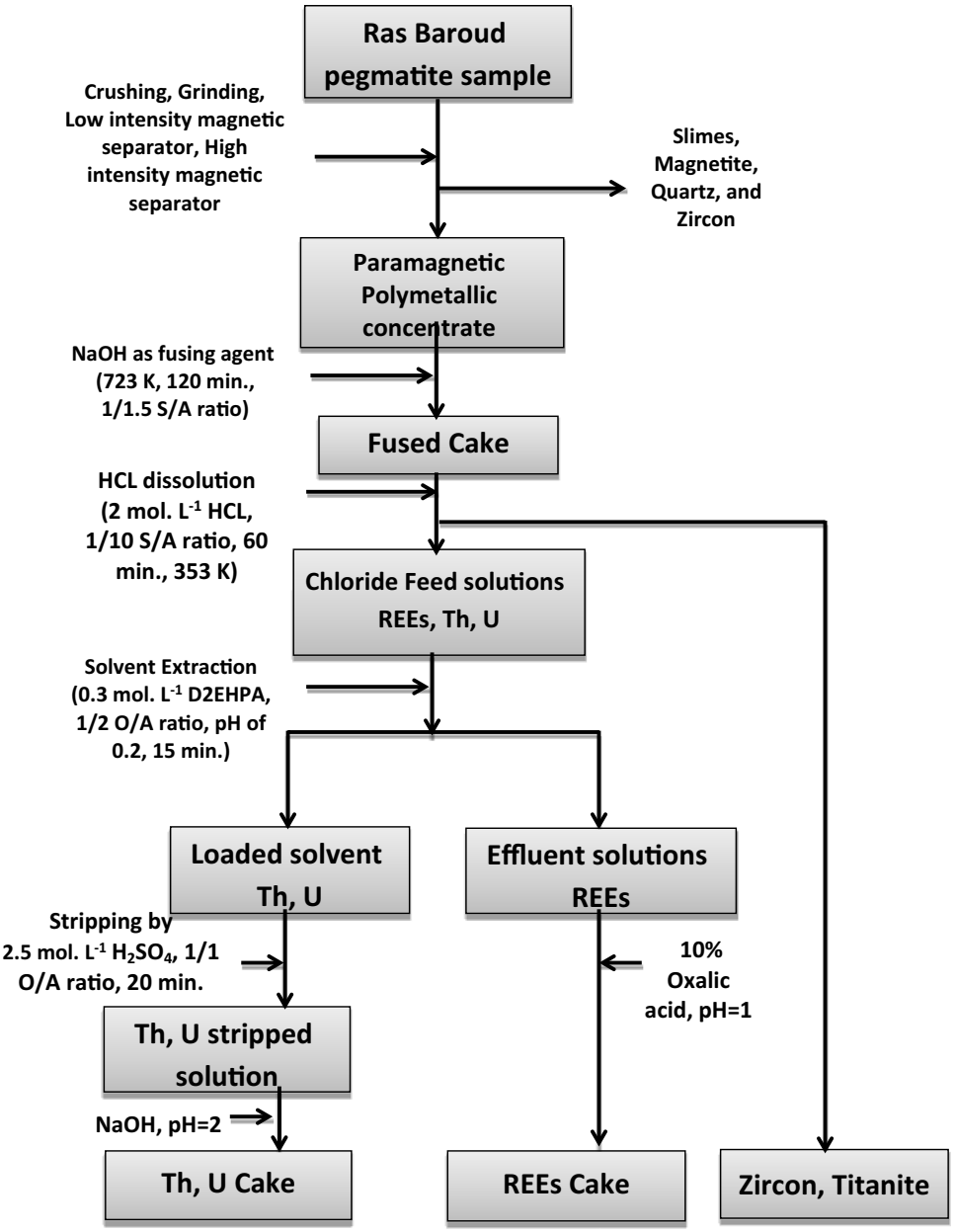

Fig. 16 A proposed flow sheet for the hydrometallurgical processing of Ras Baroud polymetallic concentrate

REE cake, which proved the successful recovery of the REEs from the radioactive actinides using D2EHPA solvent. However, more studies on the separation of individual REEs will be conducted in the future as the obtained REE cake deserves further individual processing. As shown in Fig. 16, a proposed flow sheet was drawn to collect all the recovery stages performed in this study.

4 Conclusion

Several strategic and economic rare-metal and REE-bearing minerals were recorded in the Ras Baroud pegmatite sample, and they were as follows: euxenite (Y), fergusonite (Y), yttrocolumbite, xenotime (Y), monazite (Ce), allanite, thorite, uranothorite, titanite, and Hf-zircon. The recovery of these target minerals from the head sample was performed via a low-intensity magnetic separator, followed by a high-intensity magnetic separator, and finally wet-gravity concentration via the Wilfley shaking table. Applying the optimum conditions for both separation techniques, it is possible to attain a good concentrate containing considerable contents of REE, Th, Zr, Ti, and U.

Three experimental digestion groups REEs, Th, U, Ti, and Zr were investigated using the Conceived Predictive Diagonal (CPD) technique, namely, time versus temperature, solid ore to alkali ratio versus ore particle size, and solid ore to alkali ratio versus temperature. Optimal

digestion efficiencies of 99.9, 95.6, 99.9, 52.5, and 0.47% for groups REEs, Th, U, Ti, and Zr, respectively, were attained using fusion conditions of 723 K, 120 min, 1/1.5 ore/Alkali ratio, and − 100-µm ore particle size. Fusion kinetics, isotherms, and thermodynamics were investigated using several suggested models namely pseudo reversible first order, uptake general model, and shrinking core model which matched well with the experimental digestion results. The studied models indicated that the digestion reactions for all elements were carried out through a mix of solid diffusion and chemical control.

Total actinide content was separated from the REE content using solvent extraction with di-2-ethyl hexyl phosphoric acid. About 99.9, 99.9, and 4.2% extraction efficiency for Th, U, and REEs were performed, respectively using 0.3 mol/L solvent concentration in kerosene as a diluent, 1/2 organic to aqueous ratio, aqueous pH of 0.2, and 15-min contact time. Thorium and uranium ions were stripped with a sulfuric acid solution of 2.5 mol/L, stirring time of 20 min, and *A*/*O* of 1/1 achieving 98.5 and 94.5% stripping efficiencies, respectively.

A highly purified REE precipitate was obtained from the raffinate solutions using an oxalic acid precipitation process. Th/U cake was also attained from the precipitation of stripping solutions. Solid waste from zircon-titanite mineralization has been produced by alkaline digestion.

Author Contribution Ahmed A. Eliwa: project administration, methodology, validation, formal analysis, data curation, and writing—original draft. Amal E. Mubark: methodology, formal analysis, validation, data curation, and writing—original draft. Ebrahim A. Gawad: validation, formal analysis, data curation, and writing—original draft. Ahmed H. Orabi: validation, formal analysis, visualization, writing—review and editing, and supervision. Mona M. Fawzy: methodology, validation, writing—review and editing, and project administration.

Funding Open access funding provided by The Science, Technology & Innovation Funding Authority (STDF) in cooperation with The Egyptian Knowledge Bank (EKB).

Data Availability Data will be made available on request.

Declarations

Conflict of Interest The authors declare no competing interests.

References

1. Ercit TS (2005) The classification of granitic pegmatites revisited. Can Mineral 43:129. https://doi.org/10.2113/gscanmin.43.6.2005
2. Pal D, Mishra B, Bernhardt H (2007) Mineralogy and geochemistry of pegmatite-hosted Sn-, Ta–Nb-, and Zr–Hf-bearing minerals from the southeastern part of the Bastar-Malkangiri pegmatite belt, Central India. Ore Geol Rev 30:30. https://doi.org/10.1016/j.oregeorev.2005.10.004.Pages30-55
3. Raslan M, Kharbish S, Fawzy M, El Dabe M, Fathy M (2021) Gravity and magnetic separation of polymetallic pegmatite from Wadi El Sheih Granite, Central Eastern Desert. Egypt J Min Sci 57(2):316. https://doi.org/10.15372/FTPRPI20210216
4. William S, Hanson S, Falster A (2006) Samarskite-(Yb): a new species of the samarskite group from the little patsy pegmatite, Jefferson County, Colorado. Canad Mineral 44(5):1119–1125. https://doi.org/10.2113/gscanmin.44.5.1119
5. Fawzy M, Kamar M, Saleh G (2021) Physical processing for polymetallic mineralization of Abu Rusheid mylonitic rocks, South Eastern Desert of Egypt. Int Rev Appl Sci Eng 12(2):134–146. https://doi.org/10.1556/1848.2021.00200
6. Kharbish S, Raslan M, Fawzy M, El Dabe M, Fathy M (2021) Occurrence of polymetallic mineralized pegmatite at Wadi El Sheih granite, Central Eastern Desert, Egypt. J Appl Geol Geophys 9(2):1–18. https://doi.org/10.9790/0990-0902010118
7. Kaoud MMA (1982) Conditions of formations of secondary dispersion geochemical anomalies of the rare metals in Ras Baroud, Eastern Desert. M. Sc. Thesis, Cairo University, A.R.E. 192
8. Mahdy M, Assaf H, Omer S (1991) Geological and geochemical investigation of radioactive occurrence in Gebel Ras Baroud granitic mass, Central Eastern Desert, Egypt. Proceeding of African Mining, Harare, Zimbabwe 1991:91
9. Sayyah T, Assaf H, Abdel Kader Z, Mahdy M, Omar S (1993) New Nb-Ta occurrence in ebel Ras Baroud, Central Eastern Desert. Egyptian Mineralogist 5:41–55
10. Raslan M (2009) Mineralogical and minerallurgical characteristics of samarskite-Y, columbite and zircon from stream sediments of the Ras Baroud area, Central Eastern Desert, Egypt. The Scientific Papers of the institute of Mining of The Wroclaw University of Technology, Wroclaw, Poland, Mining and Geology 128(36):179–195
11. Fawzy MM, Mahdy NM, Sami M (2020) Mineralogical characterization and physical upgrading of radioactive and rare metal minerals from Wadi Al-Baroud granitic pegmatite at the Central Eastern Desert of Egypt. Arab J Geosci 13:413. https://doi.org/10.1007/s12517-020-05381-z
12. Zhang J, Edwards C (2013) A review of rare earth mineral processing technology. Miner Process CIM J 4:38–52
13. Jordens A, Cheng YP, Waters KE (2013) A review of the beneficiation of rare earth element bearing minerals. Miner Eng 41:97–114. https://doi.org/10.1016/j.mineng.2012.10.017
14. Jordens A, Marion C, Kuzmina O, Waters KE (2014) Physicochemical aspects of allanite flotation. J Rare Earths 32(5):476–486. https://doi.org/10.1016/S1002-0721(14)60096-X
15. Abaka-Wood G, Addai-Mensah J, Skinner W (2016) Review of flotation and physical separation of rare earth element minerals. 4th UMaT Biennial International Mining and Mineral Conference MR:55–62
16. Fawzy M (2021) Flotation separation of dravite from phlogopite using a combination of anionic/nonionic surfactants, Physicochem. Probl Miner Process 57(4):87. https://doi.org/10.37190/ppmp/138587
17. Fawzy MM, Abu El Ghar MS, Gaafar IM (2022) Quaternary stream sediments, southern coast of the Red Sea, Egypt: potential

source of ilmenite, magnetite, zircon, and other economic heavy minerals. Min Metall Explor 39:655–667. https://doi.org/10.1007/s42461-022-00543-x
18. Habashi F (2013) Extractive metallurgy of rare earths. Can Metall Q 52(3):224–233
19. Abdel Wahab GM, Abdellah WM, Yousif AM, Mubark AE (2022) Preparation of pure Nb2O5 from Gabal El-Faliq Pegmatite, South Eastern Desert, Egypt. Min Metall Explor 39:833–846. https://doi.org/10.1007/s42461-019-00136-1
20. El Agamy HH, Mubark AE, Gamil EA, Abdel-Fattah NA, Eliwa AA (2023) Preparation of zirconium oxide nanoparticles from rosette concentrate using two distinct and sequential techniques: hydrothermal and fusion digestion. Chem Pap 77:3229–3240. https://doi.org/10.1007/s11696-023-02699-2
21. Xue T, Wang L, Qi T, Chu J, Qu J, Liu C (2009) Decomposition kinetics of titanium slag in sodium hydroxide system. Hydrometallurgy 95:22. https://doi.org/10.1016/j.hydromet.2008.04.004
22. Abdelgawad E (2020) A Novel technique: conceived predictive diagonal (CPD) graphical nonlinear regression modeling and simulation. J Basic Environ Sci 7:213
23. Eliwa AA, Gawad EA, Mubark AE, Abdel-Fattah NA (2021) Intensive studies for modeling and thermodynamics of fusion digestion processes of Abu Rusheid mylonite rocks. JOM 73:3419–3429. https://doi.org/10.1007/s11837-021-04837-1
24. Kawady NA, Gawad EAE, Mubark AE (2022) Modified grafted nano cellulose based bio-sorbent for uranium (VI) adsorption with kinetics modeling and thermodynamics. Korean J Chem Eng 39:408–422. https://doi.org/10.1007/s11814-021-0886-1
25. Zhu Z, Pranolo Y, Cheng C (2015) Separation of uranium and thorium from rare earths for rare earth production–a review. Miner Eng 77:185–196. https://doi.org/10.1016/j.mineng.2015.03.012
26. Pawlik C (2013) Recovery of rare earth elements from complex and low grade deposits. ALTA 2013 Uranium-REE Conference, May 25–June 1, Perth, Western Australia
27. Krebs D, Furfaro D (2013) The Kvanefjeld process. ALTA 2013 Uranium-REE Conference, May 25–June 1, Perth, Western Australia
28. Ali A, Eliwa A, Hagag M (2018) Upgrading of the crude yellowcake to a highly purified form using tris(2-ethylhexyl) phosphate in presence of EDTA or CDTA. J Environ Chem Eng 6(1):119–127. https://doi.org/10.1016/j.jece.2017.11.072
29. Zhu Z, Han Y, Luo X, Long Z, Huang X (2006) Enrichment and recovery of thorium from Baotou rare earth concentrate. In: Proceedings of 5th Academic Conference for Chinese Rare Metals, 18–19 November, Hunan Changsha, China (in Chinese)
30. Dinkar AK, Singh SK, Tripathi SC, Verma R, Reddy AVR (2012) Studies on the separation and recovery of thorium from nitric acid medium using (2-ethyl hexyl) phosphonic acid, mono (2-ethyl hexyl) ester (PC88A)/N-dodecane as extractant system. Sep Sci Technol 47:1748. https://doi.org/10.1080/01496395.2012.659786
31. Gupta CK, Malik BP, Deep A (2002) Extraction of uranium, thorium and lanthanides using Cyanex-923: their separations and recovery from monazite. J Radioanal Nucl Chem 251(3):451–456. https://doi.org/10.1023/A:1014890427073
32. Amaral JC, Morais CA (2010) Thorium and uranium extraction from rare earth elements in monazite sulfuric acid liquor through solvent extraction. Miner Eng 23:498. https://doi.org/10.1016/j.mineng.2010.01.003
33. Mohamed B, Guirguis L, Orabi A, Khalil L (2019) Extraction of thorium(IV) with N-methyl-N, N, N-trioctylammonium chloride from monazite acidic leach liquor and its use for spectrophotometric determination. Radiochemistry 61(5):569–578. https://doi.org/10.1134/S1066362219050084
34. Orabi A, Mohamed B, Ismaiel D, Elyan S (2021) Sequential separation and selective extraction of uranium and thorium from monazite sulfate leach liquor using dipropylamine extractant. Miner Eng 172:107151. https://doi.org/10.1016/j.mineng.2021.107151
35. Hung N, Thuan L, Thanh T, Thuy N, Tra D, Van K, Watanabe M, Minh P, Than H, Vuong N, Phuc D, Lee J, Jeon J, Jyothi R (2022) Selective recovery of thorium and uranium from leach solutions of rare earth concentrates in continuous solvent extraction mode with primary amine N1923. Hydrometallurgy 213:105933. https://doi.org/10.1016/j.hydromet.2022.105933
36. Singh DK, Singh H, Mathur JN (2006) Extraction of rare earths and yttrium with high molecular weight carboxylic acids. Hydrometallurgy 81:174–181. https://doi.org/10.1016/j.hydromet.2005.12.002
37. Hagag MS, Morsy AMA, Ali AH (2019) Adsorption of rare earth elements onto the phosphogypsum a waste byproduct. Water Air Soil Pollut 230:308. https://doi.org/10.1007/s11270-019-4362-z
38. Eliwa A, Mubark A (2021) Effective sorption of U(VI) from chloride solutions using zirconium silico-tungstate matrix. Int J Environ Anal Chem 103(16):4079–4097. https://doi.org/10.1080/03067319.2021.1921762
39. Mubark AE, Abd-El Razek SE, Eliwa AA, El-Gamasy SM (2023) Investigation on the sulfadiazine schiff base adsorption ability of Y(III) ions from nitrate solutions, kinetics, and thermodynamic studies. Solvent Extr Ion Exc 41(3):374–400. https://doi.org/10.1080/07366299.2023.2186180
40. Marczenko Z, Balcerzak M (2000) Analytical spectroscopy library – 10, separation, preconcentration and spectrophotometry in inorganic analysis. Elsevier Science BV, Amsterdam, The Netherlands
41. Khawassek YM, Eliwa AA, Haggag ESA et al (2019) Adsorption of rare earth elements by strong acid cation exchange resin thermodynamics, characteristics and kinetics. SN Appl Sci 1:51. https://doi.org/10.1007/s42452-018-0051-6
42. Abdel Monsif MO, El Nahas HA, Abdallah SM (2018) Mineralogy and trace elements geochemistry of pegmatite body at the northern periphery of Gabal Ras Baroud, Central Eastern Desert, Egypt. Nucl Sci Sci J 7(1):151–164. https://nssj.journals.ekb.eg/article_30736_cb0895e63312721cb1b99b3478d670d8.pdf
43. Abreu Renata D, Carlos A (2014) Morais Study on separation of heavy rare earth elements by solvent extraction with organophosphorus acids and amine reagents. Miner Eng 61:82–87. https://doi.org/10.1016/j.mineng.2014.03.015